

QUASI-BIENNIAL MODULATION OF SOLAR NEUTRINO FLUX AND SOLAR AND GALACTIC COSMIC RAYS BY SOLAR CYCLIC ACTIVITY

A. VECCHIO¹, M. LAURENZA², V. CARBONE^{1,3}, AND M. STORINI²

¹ Dipartimento di Fisica, Università della Calabria, 87036 Rende (CS), Italy; vecchio@fis.unical.it

² INAF/IFSI-Roma, 00133 Roma, Italy

³ Liquid Crystal Laboratory (INFM), 87036 Rende (CS), Italy

Received 2009 September 11; accepted 2009 November 30; published 2009 December 29

ABSTRACT

Using some solar activity indicators such as sunspot areas and green-line coronal emission during the period 1974–2001, we find that the quasi-biennial periodicity is a fundamental mode of solar variability. We provide evidence for the quasi-biennial modulation of the solar neutrino flux, thus supporting the hypothesis of a connection between solar neutrinos and solar magnetic fields, probably through direct interaction with the neutrino magnetic moment. The same periodic modulation has been detected when fluxes of solar energetic protons and galactic cosmic rays are investigated. These modulation results significantly correlate to that of the neutrino flux. Finally, the superposition of the quasi-biennial cycle to the eleven-year cycle can explain the Gnevyshev Gap phenomenon.

Key words: methods: data analysis – neutrinos – Sun: activity – Sun: particle emission

Online-only material: color figures

One of the most interesting aspects of solar physics is the cyclic behavior of magnetic activity driven by the dynamo action, usually related to the emergence of a magnetic field in active regions. Apart from the eleven-year cycle, the most prominently recognized periods are the so-called quasi-biennial oscillations (QBOs) on timescales from 1.5 yr to 3.5 yr (Rao 1973; Rieger et al. 1984; Pap et al. 1990; Bay 2003; Knaack & Stenflo 2005; Vecchio & Carbone 2008, 2009; Valdés-Galicia & Velasco 2008). This periodicity is better detected in correspondence with cycle maxima and it suffers, as the eleven-year cycle does, from period length modulation (Vecchio & Carbone 2009). Quite interestingly, corresponding QBOs also have been found in other contexts related to solar variability, such as in solar wind fluctuations, interplanetary magnetic field intensity, galactic cosmic ray (CR) flux (e.g., Valdés-Galicia et al. 1996; Kudela et al. 2002; Mursula 2004), and, more recently, in the energetic proton fluxes recorded in interplanetary space (Laurenza et al. 2009) and in the solar rotation rate (Javaraiah et al. 2009). In an early attempt to solve the puzzle of missing neutrinos (Davis & Evans 1973), the existence of a quasi-biennial modulation for solar neutrinos has been claimed (Sakurai 1979; Haubold 1998; Shirai 2004; Sakurai et al. 2008; Sturrock 2009). To date the puzzle seems to be solved in favor of neutrino flavor transformation (Masetti & Storini 1996; Fukuda 1998), thus implying a rest mass for neutrinos. Nevertheless, the origin of the QBOs and their interaction with the solar magnetic field are still debated (Bahcall & Press 1991; Oakley et al. 1994; Krauss 1991; McNutt 1995; Wilson 2000; Sturrock 2008). Modulations of neutrino flux could come either from: (1) modulations of the neutrino’s production rate by some yet unknown processes taking place inside the core of the Sun, or (2) coupling with the solar magnetic field. The latter hypothesis, if verified, would represent a confirmation of the existence of a magnetic moment for the neutrino, theoretically guaranteed by the detected neutrino’s mass. Hence, the study of short-term periodicities of the solar cycle should lead to improved knowledge of the global properties of the Sun, with particular regard to solar neutrinos and energetic particle emission.

In the present Letter, we address the topic of the existence of the quasi-biennial solar cycle and its implications by investigat-

ing the time evolution of different data sets: the Fe xv 530.3 nm coronal green line (GL) brightness and sunspot areas (SA), along with the flux of the interplanetary protons in the energy range 0.50–0.96 MeV/nucleon, measured by the Charged Particles Measurements Experiment (channel P2) aboard the *IMP 8* spacecraft and the intensity of particles measured by the Rome Neutron Monitor (NM) with a cut-off rigidity of about 6 GV.⁴ Finally we use two neutrino flux data sets, one from Homestake (ν) (a total of 108 records from 1974 to 1994; R. Davis 1994, private communication) and from super-Kamiokande (ν_K) experiments (a total of 184 records from 1996 to 2001; Fukuda 2001). The P2 data are largely representative of the low-energy solar CR flux, as the galactic contribution at energies lower than 1 MeV is practically negligible. On the other hand, NM data well represent the galactic CR flux (as the ground-level enhancements have been removed), which is modulated by the solar activity. All data sets, excluding neutrino fluxes, are monthly averaged and span 27 years from 1974 to 2001. Time evolution of the various data sets is reported in Figure 1. As a first step, we tried to identify the QBOs from the data sets through the Empirical Mode Decomposition (EMD), a technique developed to process non-stationary data (Huang et al. 1998) and successfully applied in many different contexts (Cummings et al. 2004). In the EMD framework, a time series $X(t)$ is decomposed into a finite number m of oscillating Intrinsic Mode Functions (IMFs) as

$$X(t) = \sum_{j=0}^{m-1} C_j(t) + r_m(t). \quad (1)$$

The IMFs $C_j(t)$ are a set of basis functions not assigned a priori, but rather obtained from the data set under analysis by following the procedure described by Huang et al. (1998). They represent zero mean oscillations with a characteristic timescale $\Delta\tau_j$, say

⁴ SA at <http://solarscience.msfc.nasa.gov/greenwch.shtml>; GL provided by Dr. J. Sýkora; *IMP 8* data at http://sdwww.jhuapl.edu/IMP/imp_cpme_data.html; NM at <http://www.fis.uniroma3.it/svirco/>.

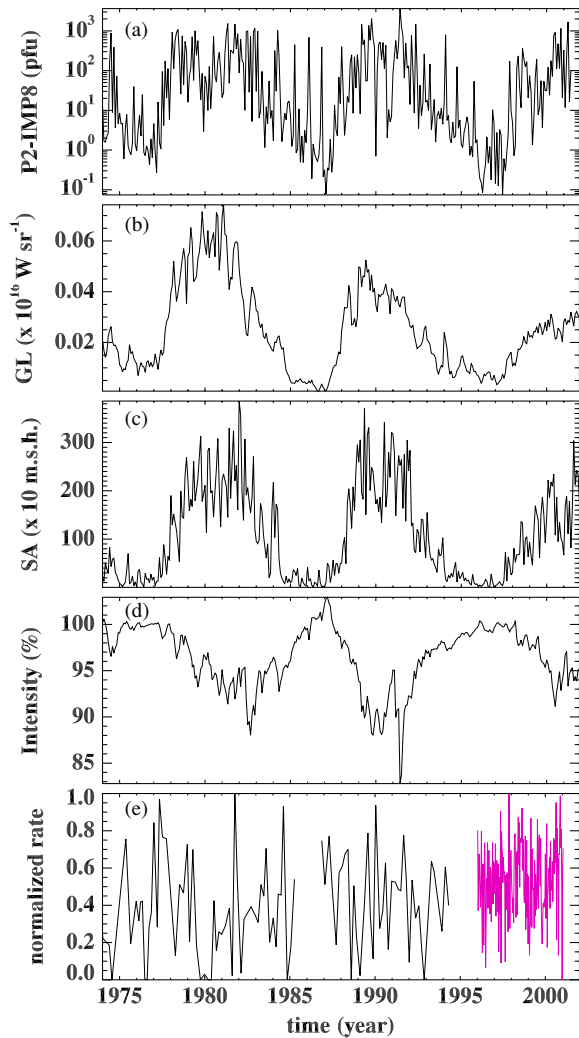


Figure 1. Time history of the P2 proton flux (a), the Fe xiv 530.3 nm coronal green line brightness (b), sunspot area (c), intensity of particles from the Rome neutron monitor (d), and neutrino fluxes (e) from Homestake (black line) and Super-Kamiokande (purple line) experiments.

(A color version of this figure is available in the online journal.)

the average spacing between extrema of the data. The IMFs are not restricted to a particular frequency but can experience both amplitude and frequency modulation. The residue $r_m(t)$ in Equation (1) describes the mean trend. This kind of decomposition is local, complete, and orthogonal; the orthogonality can be exploited to reconstruct the signal through partial sums in Equation (1) (Huang et al. 1998; Cummings et al. 2004; McDonald et al. 2007; Terradas et al. 2004). The statistical significance of information content for the IMFs with respect to a white noise can be checked by applying the test by Wu & Huang (1996) based on the following argument. When EMD is applied to a white noise series, the constancy of the product between the energy density of each IMF and its corresponding averaged period can be deduced. This relation can be used to derive the analytical energy density spread function of each IMF as a function of different confidence levels. Thus, by comparing the energy density of the IMFs extracted from the actual data with the theoretical spread function, one can distinguish IMFs containing information at the selected confidence level from purely noisy IMFs. By applying EMD to our data sets, we found one IMF oscillating at $\Delta\tau_j \simeq 11$ yr, which defines the basic solar cycle mode. In addition, IMFs, oscillating with timescales in the range $1.4 \text{ yr} \leq$

$\Delta\tau_j \leq 4$ yr, are obtained for each data set. They are used to reconstruct the QBOs through partial sums in Equation (1). Their amplitudes are all above the 90% confidence level with respect to a white noise, with the exception of super-Kamiokande modes for which the confidence level is 75%. Further IMFs can be associated with other solar cycle periodicities, secular variations and noise. In particular, while QBOs and the eleven-year period are common to all data sets, particle time series (P2, NM, and ν) also show a significant typical timescale of about 7 yr. In Table 1, we report the information about the obtained EMD modes. The C_6 mode for NM data has an opposite phase with respect to GL, SA, and P2, which represents the well-known anti-correlation of CRs with respect to the eleven-year cycle of solar activity. The C_5 mode for ν flux has an average period of about $\Delta\tau_5 \simeq 13$ yr, which perhaps could be classified within the period-length modulation of the eleven-year cycle (Vecchio & Carbone 2009), although it is noticeably out of phase with all other eleven-year modes. In the present Letter we focus on QBOs, while a detailed analysis of the complete set of EMD modes will be reported in a future work. Time evolution of both QBOs and the eleven-year cycle for P2, GL, and SA data is reported in panels (a) and (b) of Figure 2, respectively. It is worthwhile to mention that our analysis about QBOs allows new information on the generation of the so-called Gnevyshev Gap (GG), defined as the time interval, during the maximum activity phase of each eleven-year cycle, in which a decrease in solar activity is observed; namely, the cycles have structured maxima, generally with a first peak at the end of the increasing phase and a second one at the start of the declining phase (see for a review Storini et al. (2003) and references therein). From panel (c) of Figure 2, we demonstrate that the superposition of the QBOs and the eleven-year cycle produces the GG feature, as conjectured in the past (Benevolenskaya 1998; Bazilevskaya et al. 2000). We also confirm that the amplitudes (see Figure 2 panel (a) and Figure 3) of the QBOs are enhanced around the years of maximum solar activity (Bazilevskaya et al. 2000; Mursula & Zieger 2000; Valdés-Galicia & Velasco 2008).

After identifying the QBO components through the EMD from the different indicators, they are compared by means of correlative analyses. As expected, the strongest values of correlation are found around the solar cycle maxima where the QBO amplitudes are higher. In particular, in Table 2 we report the Pearson correlation coefficients $r_{X,Y}$ between QBO signals for couples of parameters X and Y , obtained for a time interval lasting 1.5 yr around the times $T_{21} = 1980.25$ and $T_{22} = 1990.75$ for cycle 21 and cycle 22, respectively. Note that T_{21} and T_{22} correspond to the GG times derived from the P2 time series, for which the GG is more clearly apparent. When dealing with correlation between EMD modes, the Pearson coefficient is commonly used (Cummings et al. 2004). Nevertheless, there is no standard method for determining the significance of cross-correlations between single EMD modes or signals obtained through partial sums. In order to estimate the significance of the correlation coefficients, three independent statistical tests have been performed based on Fisher's transformation, bootstrap, and random phases approaches. Results are shown in Table 2, where Δr_F represents the 95% Fisher's confidence interval for the correlation coefficient. In the bootstrap analysis, Pearson's correlation coefficient r has been calculated for 10,000 different realizations of x - and y -parameters obtained through a resample of the original time series by picking an arbitrary set of subsamples (having the same number of data points) with replacements (i.e., an element may appear multiple times in a given bootstrap sample). By building the r histogram, the

Table 1
Information About the Obtained EMD Modes

Parameter	m	Eleven-year IMF	QBO IMFs	QBO Periods (yr)
GL	7	C_5	$C_3 + C_4$	$\tau_3 = 1.5 \pm 0.1$; $\tau_4 = 3.4 \pm 0.2$
SA	8	C_6	$C_4 + C_5$	$\tau_4 = 2.4 \pm 0.1$; $\tau_5 = 3.7 \pm 0.2$
P2	9	C_7	$C_4 + C_5$	$\tau_4 = 1.7 \pm 0.1$; $\tau_5 = 2.9 \pm 0.2$
NM	8	C_6	$C_3 + C_4$	$\tau_3 = 1.4 \pm 0.1$; $\tau_4 = 2.3 \pm 0.3$
ν	6	C_5 (?)	$C_2 + C_3$	$\tau_2 = 1.9 \pm 0.1$; $\tau_3 = 2.2 \pm 0.2$
ν_K	7	...	$C_5 + C_6$	$\tau_5 = 1.6 \pm 0.1$; $\tau_6 = 2.5 \pm 0.1$

Notes. Number (m) of EMD modes in Equation (1) for each data set; significant modes for the eleven-year cycle and QBOs along with their typical periods, calculated as the average time difference between local extrema. The standard error is provided for each period.

Table 2
Results of Correlative Analysis

$X-Y$	Cycle 21				Cycle 22			
	$r_{X,Y}$	Δr_F	Δr_{boot}	P_{rp}	$r_{X,Y}$	Δr_F	Δr_{boot}	P_{rp}
GL-SA	-0.47	[-0.76, -0.02]	[-0.76, 0.05]	0.30	0.98	[0.95, 0.99]	[0.97, 0.99]	0.01
P2-SA	0.18	[0.06, 0.59]	[-0.35, 0.60]	0.42	0.50	[0.06, 0.78]	[0.02, 0.77]	0.28
P2-GL	-0.73	[-0.89, -0.41]	[-0.92, -0.24]	0.14	0.60	[0.20, 0.83]	[0.10, 0.83]	0.20
P2-NM	-0.98	[-0.99, -0.95]	[-0.99, -0.97]	0.01	-0.92	[-0.97, -0.80]	[-0.96, -0.85]	0.03
SA- ν	0.10	[0.04, 0.53]	[-0.55, 0.57]	0.47	0.17	[0.07, 0.58]	[-0.31, 0.58]	0.43
GL- ν	-0.77	[-0.91, -0.49]	[-0.97, -0.23]	0.14	0.30	[0.18, 0.66]	[-0.20, 0.70]	0.37
P2- ν	0.96	[0.90, 0.98]	[0.91, 0.98]	0.01	0.93	[0.82, 0.97]	[0.82, 0.97]	0.03
NM- ν	-0.90	[-0.96, -0.75]	[-0.95, -0.78]	0.06	-0.99	[-0.99, -0.97]	[-0.99, -0.98]	0.01

Notes. Pearson correlation coefficients $r_{X,Y}$ between the QBOs of different couples of parameters X and Y during the maximum phases of cycles 21 and 22. Δr_F and Δr_{boot} represent the 95% confidence intervals for the correlation coefficient from Fisher's and bootstrap tests, respectively. P_{rp} indicates the probability, calculated through the random phases test, to obtain correlation values greater than $r_{X,Y}$ due to chance.

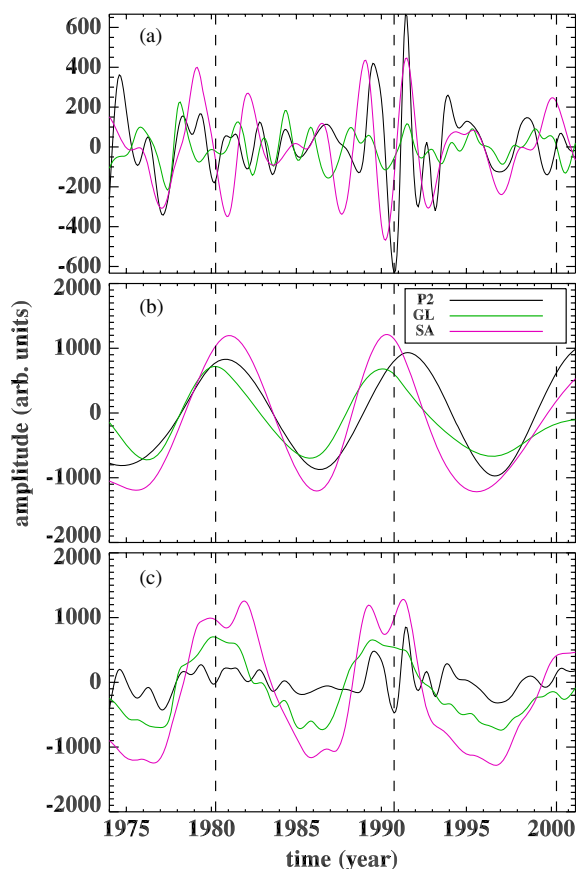


Figure 2. EMD reconstruction of both (a) QBOs and (b) eleven-year cycle for P2, GL, and SA, and (c) superposition of QBOs and eleven-year. Dashed lines indicate the time around which correlations are calculated.

(A color version of this figure is available in the online journal.)

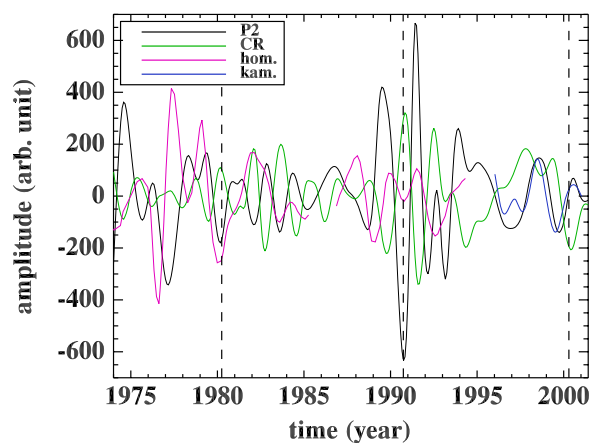


Figure 3. QBO reconstructed through the EMD for P2, NM, and neutrino fluxes. Dashed lines indicate the time around which correlations are calculated.

(A color version of this figure is available in the online journal.)

95% confidence interval Δr_{boot} for the correlation coefficient can be estimated. Finally, the random phases method (Simpson et al. 2001) allows one to compute the r histogram from 10,000 realizations of x, y obtained by randomizing the phases and keeping the amplitudes unchanged. The significance of Pearson's coefficient $r_{X,Y}$ can be estimated by summing up the values for $r > r_{X,Y}$ thus indicating the probability P_{rp} to obtain r values greater than $r_{X,Y}$ by chance.

While the eleven-year components are not perfectly in phase in both cycles (Figure 2(b)), a striking result is that QBOs for P2, GL, and SA are significantly correlated in cycle 22, while they are out of phase in cycle 21. It follows that the GG is almost synchronous and well shaped in cycle 22 for all the considered parameters, which is consistent with previous

findings (Bazilevskaya et al. 2000). We have to consider that the sunspot area is a proxy strictly related to the emergence of active regions on the solar photosphere whereas the GL brightness is more sensitive to changes in the configuration of the global magnetic field and the emission of solar CRs involves shock formation in the solar corona (e.g., Reames et al. 1999) or post-Coronal Mass Ejection reconnection processes (Cane et al. 1999; Klein & Posner 2005). Hence, the QBO behavior in cycle 21 results in non-synchronous multi-peaked or rather shallow two-peaked solar maxima observed for many parameters (Storini & Pase 1995; Feminella & Storini 1997; Storini et al. 2003; Bazilevskaya et al. 2000). In particular, we find that GGs in the P2 flux and SA are shifted in time similarly to the yearly number of SEP events and SA in cycle 21 (Bazilevskaya et al. 2006). This should be interpreted as the result of gross changes in the topology of the interplanetary magnetic field (van Allen 1988) and/or the incidence and intensity of magnetic discontinuities, which were associated with the reversal of polarity of the Sun's polar magnetic field during 1979–1981 (Rodríguez-Pacheco et al. 1997).

In order to clarify the last topic, we analyzed the variability of the galactic CR intensity, which are strongly influenced by the variations of the global magnetic field of the Sun. The QBOs have been clearly detected through the EMD technique in the NM data, as displayed in Figure 3. A significant anti-correlation $r_{P2,NM} = -0.59$ between the QBOs of P2 and NM is obtained throughout the whole period 1974–2001. The correlation is even stronger during the maximum phases (see Table 2). An anti-correlation between solar and galactic CRs, although well known for the eleven-year component, has never been detected in this range of frequency. This strong anti-correlation represents an indirect confirmation of the existence of the quasi-biennial cycle in the evolution of the solar magnetic field, which affects the two CR populations in opposite ways.

A surprising result comes from the clear observation of QBOs also for neutrino fluxes (cf. Figure 3). While the existence of quasi-biennial modulation in solar neutrino flux has been claimed from several experiments (Sakurai et al. 2008) its correlation with the solar activity has never been absolutely proved. We remark that, since the solar indicator signals are dominated by the eleven-year period of the main cycle, QBOs in rough data cannot be directly correlated with those eventually present in neutrino fluxes, but usually running means or smoothing procedures are applied (Masetti & Storini 1996; Boyer et al. 2000). Moreover, it has been claimed that when an indicator exhibits the eleven-year periodicity, no reliable values of correlations could be obtained (Walther 1997). On the contrary, in the present Letter, the EMD is used as a filter to isolate (by partial sums of single IMFs) the QBOs contribution from the rough time series and their correlation is directly calculated without averages or smoothing.

We find a strong positive (negative) correlation between the QBO of the Homestake neutrino flux and the corresponding P2 (NM) mode, mainly evident at the solar maxima. According to the performed tests, the correlations are significant (Table 1). This indicates that a strong magnetic field is perhaps necessary to affect the neutrino flux. No correlations between neutrino flux and SA and GL are found. By considering also the QBO relative to the super-Kamiokande data set (Figure 3), we observe a strong correlation between ν_K and both P2 and NM fluxes, namely $r_{\nu_K,P2} = 0.94$ ($\Delta r_F = [0.85, 0.98]$, $\Delta r_{boot} = [0.89, 0.97]$ and $P_{TP} = 0.006$) and $r_{\nu_K,NM} = -0.92$ ($\Delta r_F = [-0.97, -0.80]$, $\Delta r_{boot} = [-0.97, -0.78]$ and $P_{TP} = 0.01$), respectively, during

a period lasting 1.5 yr around the time $T_{23} = 2000.3$, say the time of cycle 23 maximum as indicated on the NOAA Web site.

As a conclusion, the QBOs are a fundamental mode of solar activity that greatly affect the fluxes of both solar and galactic CRs and neutrinos. In particular, our findings represent strong evidence of a relationship between solar neutrino flux and solar activity. Our approach is somewhat different from earlier attempts where the neutrino flux, dominated by QBOs, was directly compared with the eleven-year solar cycle described by SA or sunspot numbers, which cannot represent the complexity of the solar magnetic cycle. On the contrary, we compare the proper oscillating components of the solar cycle at the same time scale, selected through EMD. Since the modulations of both NM and P2 are driven by the solar magnetic field, the strong correlation found between neutrinos and the two populations of CRs suggests that the magnetic flux plays a crucial role in the modulation of the solar neutrino flux as well, probably involving magnetic moment interactions through the spin-flavor precession (Voloshin & Vysotskii 1986).

We thank the referee for useful comments. This work was partially supported by ASI/INAF contracts I/090/06/0 and I/015/07/0, by INAF (PRIN 2007) “Scientific exploitation of the Interferometric Bidimensional Spectrometer (IBIS) Magnetic structuring of the lower solar atmosphere.” Thanks are due to PNRA for the use of the RAC-ANT database.

REFERENCES

- Bahcall, J. N., & Press, W. H. 1991, *ApJ*, **370**, 730
 Bay, T. 2003, *ApJ*, **591**, 406
 Bazilevskaya, G. A., Krainev, M. B., Makhmutov, V. S., Flückiger, E. O., Sladkova, A. I., & Storini, M. 2000, *Sol. Phys.*, **197**, 157
 Bazilevskaya, G. A., Makhmutov, V. S., & Sladkova, A. I. 2006, *Adv. Space Res.*, **38**, 484
 Benevolenskaya, E. E. 1998, *ApJ*, **509**, L49
 Boyer, J., Hahn, R. L., & Cumming, J. B. 1986, *ApJ*, **537**, 1080
 Cane, H. V., Erickson, W. C., & Prestage, N. P. 2002, *J. Geophys. Res.*, **107**, 14
 Cummings, D. A. T., et al. 2004, *Nature*, **427**, 344
 Davis, R., Jr., & Evans, J. C. 1973, Proc. 13th ICRC (Denver), **3**, 2001
 Feminella, F., & Storini, M. 1997, *A&A*, **322**, 311
 Fukuda, S., et al. 2001, *Phys. Rev. Lett.*, **86**, 5651
 Fukuda, Y., et al. 1998, *Phys. Rev. Lett.*, **81**, 1562
 Haubold, H. J. 1998, *Ap&SS*, **258**, 201
 Huang, N. E., et al. 1998, *Proc R. Soc. Lond. A*, **454**, 903
 Javaraiah, J., Ulrich, R. K., Bertello, L., & Boyden, J. E. 2009, *Sol. Phys.*, **257**, 61
 Klein, K.-L., & Posner, A. 2005, *A&A*, **438**, 1029
 Knaack, R., & Stenflo, J. O. 2005, *A&A*, **438**, 349
 Krauss, L. M. 1991, *Nature*, **348**, 403
 Kudela, K., Rybak, J., Antalová, A., & Storini, M. 2002, *Sol. Phys.*, **205**, 165
 Laurenza, M., Storini, M., Giangravé, S., & Moreno, G. 2009, *J. Geophys. Res.*, **114**, A01103
 Masetti, S., & Storini, M. 1996, *ApJ*, **472**, 827
 McDonald, A. J., Baumgaertner, A. J. G., Fraser, G. J., George, S. E., & Marsh, S. 2007, *Ann. Geophys.*, **25**, 375
 McNutt, R. L. 1995, *Science*, **270**, 1635
 Mursula, K., & Vilppola, J. H. 2004, *Sol. Phys.*, **221**, 337
 Mursula, K., & Zieger, B. 2000, *Adv. Space Res.*, **25**, 1939
 Oakley, D. S., Snodgrass, H. B., Ulrich, R. K., & Van De Kop, T. L. 1994, *ApJ*, **437**, L63
 Pap, J., Tobiska, W. K., & Bouwer, S. D. 1990, *Sol. Phys.*, **129**, 165
 Rao, K. R. 1973, *Sol. Phys.*, **29**, 47
 Reames, D. V., Ng, C. K., & Tylka, A. J. 1999, *Geophys. Res. Lett.*, **26**, 3585
 Rieger, E., Kanbach, G., Reppin, C., Share, G. H., Forrest, D. J., & Chupp, E. L. 1984, *Nature*, **312**, 623
 Rodríguez-Pacheco, J., Sequeiros, J., del Peral, L., Medina, J., & Wenzel, K.-P. 1997, *J. Geophys. Res.*, **102**, 9801
 Sakurai, K. 1979, *Nature*, **278**, 146

- Sakurai, K., Haubold, H. J., & Shirai, T. 2008, *Space Rad.*, 5, 207
- Shirai, T. 2004, *Sol. Phys.*, 222, 199
- Simpson, D. M., Infantosi, A. F. C., & Botero Rosas, D. A. 2001, *Med. Biol. Eng. Comput.*, 39, 428
- Storini, M., Bazilevskaya, G. A., Fluckiger, E. O., Krainev, M. B., Makhmutov, V. S., & Sladkova, A. I. 2003, *Adv. Space Res.*, 31, 895
- Storini, M., & Pase, S. 1995, *STEP GBRSC News*, 5, 255 (special issue)
- Sturrock, P. A. 2008, *ApJ*, 688, L53
- Sturrock, P. A. 2009, *Sol. Phys.*, 254, 227
- Terradas, J., Oliver, R., & Ballester, J. L. 2004, *ApJ*, 614, 435
- Valdés-Galicia, J. F., Perez-Enriquez, R., & Otaola, J. A. 1996, *Sol. Phys.*, 167, 409
- Valdés-Galicia, J. F., & Velasco, V. M. 2008, *Adv. Space Res.*, 41, 297
- van Allen, J. A. 1988, *Geophys. Res. Lett.*, 15, 1527
- Vecchio, A., & Carbone, V. 2008, *ApJ*, 683, 536
- Vecchio, A., & Carbone, V. 2009, *A&A*, 502, 981
- Voloshin, M. B., & Vysotskii, M. I. 1986, *Sov. J. Nucl. Phys.*, 44, 544
- Walther, G. 1997, *Phys. Rev. Lett.*, 79, 23
- Wilson, R. M. 2000, *ApJ*, 545, 532
- Wu, Z., & Huang, N. E. 2004, *Proc. R. Soc. Lond. A*, 460, 1597